

Dynamics and stability of Purcell's three-link microswimmer near a wall

Yizhar Or*

Faculty of Mechanical Engineering, Technion - Israel Institute of Technology, Israel

(Dated: September 13, 2010)

The motion of swimming microorganisms is strongly influenced by the presence of boundaries. Attraction of bacteria and sperm cells to surfaces is a well-known phenomenon which has been observed in experiments and confirmed by numerical simulations. The paper studies this effect from a viewpoint of dynamical systems theory by analyzing a swimmer model which is a variant of the classical Purcell's three-link swimmer near an infinite plane wall. The underlying geometric structure of the swimmer's dynamics and its relation to stability are elucidated. It is found that a swimmer which breaks its fore-aft symmetry has a preferred swimming direction in which its motion is passively stable and converges to a fixed separation distance from the wall.

PACS numbers: 47.63.mf, 47.63.Gd, 47.10.Fg, 11.30.Er

The motion of swimming microorganisms is governed by low-Reynolds-number (Re) hydrodynamics, where viscous effects dominate and inertial effects are negligible [1]. Many works study theoretical models of low- Re locomotion in which the swimmer undergoes non-reciprocal shape changes, e.g. [2]. A classical example is Purcell's 30-years-old model of an articulated three-link swimmer [3]. In the last decade, the dynamics of Purcell's swimmer has been formulated by using resistive force theory in [4], optimization of its motion has been studied in [5], and the geometric structure of its governing dynamic equations has been investigated in [6]. While these works focus on *unbounded fluid domain*, it is known that boundary effects have profound influence on the dynamic behavior and motion trajectories of swimming microorganisms [7]. In particular, such swimmers are often attracted to solid boundaries, a phenomenon that has been observed in experiments [8, 9] and confirmed in numerical hydrodynamic simulations [10]. Simplified theoretical models of low- Re swimmers near a wall has been recently proposed in order to study this effect, e.g. [11, 12]. In particular, the work in [12] considered simplified models of swimmers with a fixed shape which are composed of interconnected rotating spheres. The stability of swimming near a wall was studied, and particularly its relation to geometric symmetries of the dynamic equations. These results were recently demonstrated in motion experiments of macro-scale low- Re robotic swimmers [13].

The goal of this work is to extend the analysis in [12] to the shape-changing swimmer model of Purcell and study the dynamics and stability of its motion near an infinite plane wall by analyzing the geometric structure of the dynamic equations. In particular, we focus on a class of periodic shape changes that induce a *reversing symmetry* [14] on the swimmer's continuous-time and discrete-time dynamics, and show that the resulting net motion parallel to the wall possesses marginal dynamic stability which is associated with nearly periodic oscillations under perturbations. We then show that breaking the reversing symmetry results in net motion parallel to the

wall which is asymptotically stable (i.e. attractive) when traveling in a preferred direction, in agreement with the observations in [9].

The classical model of Purcell's three-link swimmer in unbounded fluid is shown in Fig. 1(a). The swimmer consists of three elongated links, and changes its shape by controlling the inter-link angles ϕ_1 and ϕ_2 . In order to formulate the dynamics of this swimmer, let $\mathbf{q} = (x, y, \theta)^T$ denote the planar position and orientation of the swimmer's central link, and denote $\mathbf{s} = (\phi_1, \phi_2)^T$. The relation between the swimmer's instantaneous velocity $\dot{\mathbf{q}}$ and the rate-of-change of its shape $\dot{\mathbf{s}}$ takes the form

$$\dot{\mathbf{q}} = \mathbf{G}(\mathbf{q}, \mathbf{s})\dot{\mathbf{s}}. \quad (1)$$

Typically, the shape of the swimmer is changed in time as a prescribed periodic function $\mathbf{s}(t)$, called *gait*, in order to generate net motion of the swimmer $\mathbf{q}(t)$. In unbounded fluid domain, the relation (1) has a simplifying geometric structure called *gauge symmetry* [6, 15], meaning that the swimmer's motion does not depend on its absolute position and orientation. Fig. 1(b) shows the classical gait analyzed in [3, 4], which forms a symmetric square loop in (ϕ_1, ϕ_2) -plane. Due to the symmetry implied by the equal lengths of the two distal links, it was shown that changing ϕ_1 and ϕ_2 along this loop results in net sideways motion of the swimmer along the axis of the central link.

When the swimmer moves in a bounded fluid domain, it interacts with the boundary in a very complicated way. The simplified model of local resistive coefficients for slender bodies which was used in [4] does not admit a direct generalization that accounts for boundary effects except for very limited situations [16]. Thus, this work considers a variant of Purcell's swimmer model, where the slender links are replaced by a chain of ten identical spheres of equal radius $a = 1$ connected by thin rods, such that the center-center spacing between two neighboring spheres is $4a$ [Fig. 1(c)]. The swimmer is placed near an infi-

nite planar wall located at $y = 0$. Under this simplified model, the swimmer's equation of motion (1) can be derived by using the far-field resistance tensor developed in [17], which accounts for the hydrodynamic interaction of multiple spheres and a plane wall (see [18] for a detailed derivation of (1)). Due to the presence of a boundary, the gauge symmetry no longer holds, so that under a given shape change $\mathbf{s}(t)$, the net motion of the swimmer strongly depends on its pose \mathbf{q} . When the shape change $\mathbf{s}(t)$ repeats itself in a cyclic fashion (i.e. a fixed gait), the swimming equation (1) induces a discrete-time dynamical system

$$\mathbf{q}_{k+1} = \mathcal{F}(\mathbf{q}_k), \quad (2)$$

where $k \in \mathbb{N}$ is the discrete time and \mathbf{q}_k is the solution of the continuous-time equation (1) evaluated at time instants $t = kT$ and T is the period of the gait. As a particular example, we simulate the dynamic motion of the swimmer in Fig. 1(c) under the symmetric square gait shown in Fig. 1(b), starting at $\mathbf{q}(0) = (0, 10, 0^\circ)$ and $\phi_1(0) = \phi_2(0) = \alpha$, where $\alpha = 60^\circ$. Snapshots of the swimmer's pose $\mathbf{q}(t)$ at times $t = 10kT$ (i.e. every ten gait cycles) are shown in Fig. 1(d). The continuous-time trajectory of the center of the swimmer's middle link for the first 10 cycles is plotted as a dashed curve. It can be seen that on top of the swimmers inherent undulations, its average motion includes rotation and deviation away from the wall. This example motivates the following two key questions: First, does there exist a gait for this swimmer model that generates net (average) motion of translation parallel to the wall? Second, can this parallel motion be *dynamically stable* under a fixed gait? That is, given an initial perturbation in the swimmer's pose, will it converge to the same trajectory of steady parallel translation?

In order to address these questions, we first study the geometric structure of the swimmer's dynamic equations. Since the wall extends along the infinite line $y = 0$, it is clear that equation (1) is invariant under shifting the swimmer parallel to the wall, that is, $\mathbf{G}(\mathbf{q}, \mathbf{s})$ is independent of x . Defining the reduced pose $\mathbf{q}' = (y, \theta)$, equation (1) can be reduced to

$$\dot{\mathbf{q}}' = \mathbf{G}'(\mathbf{q}', \mathbf{s})\dot{\mathbf{s}}, \quad (3)$$

where $\mathbf{G}'(\mathbf{q}', \mathbf{s})$ is the lower 2×2 submatrix of $\mathbf{G}(\mathbf{q}, \mathbf{s})$ in (1). Similarly, in the discrete-time dynamics (2), $\mathcal{F}(\mathbf{q})$ is also independent of x , and (2) can be reduced to

$$\mathbf{q}'_{k+1} = \mathcal{F}'(\mathbf{q}'_k), \quad (4)$$

where $\mathcal{F}'(\cdot)$ takes the (y, θ) -components of $\mathcal{F}(\cdot)$ in (2). Therefore, a net motion of translation parallel to the wall is simply described by a *fixed point* \mathbf{q}'_e of the reduced discrete-time dynamics (4), such that $\mathcal{F}'(\mathbf{q}'_e) = \mathbf{q}'_e$.

Another key property of the three-link swimmer which

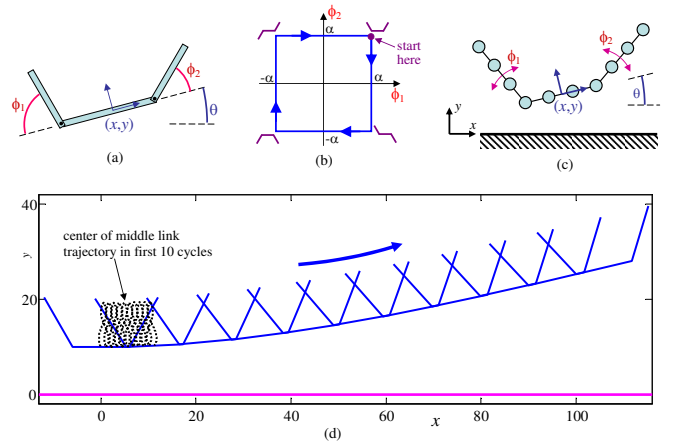


FIG. 1: (a) Purcell's three-link swimmer model. (b) Symmetric square gait in (ϕ_1, ϕ_2) -plane. (c) The chain-of-spheres three-link swimmer model near a wall. (d) Motion snapshots near a wall under the symmetric square gait.

is a consequence of the equal length of its two distal links is a reflection symmetry about the line bisecting the middle link. When the swimmer is placed near the infinite plane wall at $y = 0$, this reflection symmetry implies the following relation on the matrix $\mathbf{G}(\mathbf{q}, \mathbf{s})$ in (1):

$$\mathbf{G}(\mathbf{M}_q \mathbf{q}, \mathbf{M}_s \mathbf{s}) = \mathbf{M}_q \mathbf{G}(\mathbf{q}, \mathbf{s}) \mathbf{M}_s,$$

$$\text{where } \mathbf{M}_q = \text{diag}(-1, 1, -1) \text{ and } \mathbf{M}_s = \begin{pmatrix} 0 & 1 \\ 1 & 0 \end{pmatrix}. \quad (5)$$

In words, (5) simply means that reflecting the pose of the middle link about the y -axis ($\mathbf{M}_q \mathbf{q}$) and interchanging between the left and right links ($\mathbf{M}_s \mathbf{s}$) is equivalent to reflecting the entire swimmer about the y -axis. In order to establish an analogous relation for the discrete-time dynamics (2), we now define a special class of gaits as follows. A T -periodic gait $\mathbf{s}(t)$ such that $\mathbf{s}(0) = \mathbf{s}(T)$ is called *reversing-symmetric* if

$$\mathbf{s}(\frac{1}{2}T - t) = \mathbf{M}_s \mathbf{s}(\frac{1}{2}T + t) \text{ for all } t \in [0, \frac{1}{2}T], \quad (6)$$

where \mathbf{M}_s is defined in (5). Geometrically, (6) implies that the gait loop in (ϕ_1, ϕ_2) -plane is symmetric with respect to the line $\phi_1 = \phi_2$, while the start point $\mathbf{s}(0)$ also lies on this line [Fig. 2(a)]. The physical meaning of a reversing symmetric gait is that playing the gait backward in time is equivalent to interchanging between the left and right links. Under this class of reversing-symmetric gaits, the discrete-time dynamics of the swimmer in (2) satisfies the following relation

$$\mathcal{F}(\mathbf{M}_q \mathbf{q}) = \mathbf{M}_q \mathcal{F}^{-1}(\mathbf{q}), \quad (7)$$

where \mathbf{M}_q is defined in (5). A relation of the form (7) on $\mathcal{F}(\cdot)$ is called a *reversing symmetry* [14] of the discrete-time dynamical system (2). Physically, it means that a

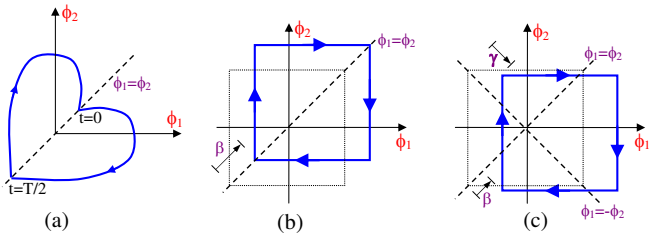


FIG. 2: (a) A reversing-symmetric gait in (ϕ_1, ϕ_2) -plane. (b) The square gait shifted along the line $\phi_1 = \phi_2$. (c) The square gait shifted along the lines $\phi_1 = \phi_2$ and $\phi_1 = -\phi_2$.

swimmer which is reflected about the y axis will swim along a reflected trajectory, but in reversed direction. This is the analogue of the continuous-time reversing symmetry of the two-rotating-spheres swimmer in [12].

A key consequence of the notion of reversing-symmetric gaits is the existence of fixed points of (4). This stems from the following observation. Consider the reduced dynamics of the three-link swimmer in (3) under a reversing-symmetric gait $\mathbf{s}(t)$ and initial condition $\mathbf{q}'(0) = (y_0, 0)$. If the solution after a half-cycle $\mathbf{q}'(t = \frac{1}{2}T)$ satisfies $\theta(\frac{1}{2}T) = 0$, then $\mathbf{q}'(T) = (y_0, 0)$, resulting in a fixed point $\mathbf{q}'_e = (y_0, 0)$ of (4) under the gait $\mathbf{s}(t)$. The explanation relies on the fact that the half-cycle pose $\mathbf{q}'(\frac{1}{2}T) = (y_0 + \Delta y, 0)$ is invariant under the y -axis mirror reflection, i.e. $\mathbf{q}'(\frac{1}{2}T) = \mathbf{M}'_q \mathbf{q}'(\frac{1}{2}T)$, where $\mathbf{M}'_q = \text{diag}(1, -1)$. Therefore, relations (5) and (6) imply that the trajectory $\mathbf{q}'(t)$ in the second half-cycle is precisely a mirror reflection of the first half-cycle trajectory, but in reversed time. Thus, the change in $y(t)$ during the second half-cycle is exactly $-\Delta y$. Moreover, it can be shown that the change in the x -component over the first half-cycle is *doubled* in the second half-cycle, so that a full gait cycle results in pure translational motion along the wall in the x -direction. As a result, finding a reversing-symmetric gait that induces an equilibrium point $\mathbf{q}'_e = (y_e, 0)$ of (4) reduces to finding a half-cycle $\mathbf{s}(t)$ with start and end points lying on the line $\phi_1 = \phi_2$ that generates *zero rotation only* $\theta(\frac{1}{2}T) = 0$. As an example, consider the symmetric square gait of Fig. 1(b), which is obviously a reversing-symmetric gait. In the presence of the wall, this gait will, in general, result in nonzero rotation, as demonstrated in the simulation of Fig. 1(d). Nevertheless, it is possible to modify the gait in a way that preserves its reversing symmetry such that it generates a counter-rotation which exactly cancels the wall-induced rotation. An easy way for doing so is to shift the entire square loop in (ϕ_1, ϕ_2) -plane in an amount of β along the diagonal line $\phi_1 = \phi_2$ [Fig. 2(b)]. Thus, for any given distance from the wall y_e , one can assign a shift β which results in a reversing-symmetric gait that induces an equilibrium point $\mathbf{q}'_e = (y_e, 0)$ of (4), corresponding to net parallel translation along the wall at a distance y_e . For example, numerical simulations for the

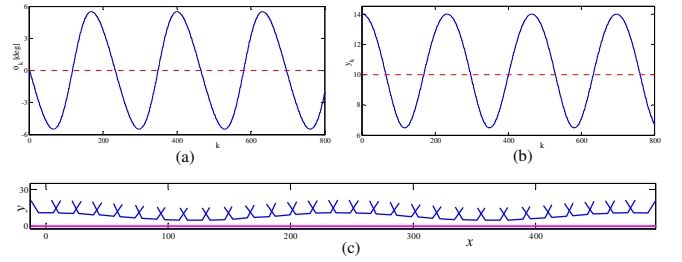


FIG. 3: Simulation of the reversing-symmetric motion. (a) Plot of y_k . (b) Plot of θ_k . (c) Snapshots of the swimmer's motion near the wall.

chain-of-spheres three-link swimmer of Fig. 1(c) reveal that a square gait of amplitude $\alpha = 60^\circ$ with a shift of $\beta = -1.276^\circ$ induces a steady translation parallel to the wall at a distance $y_e = 10$.

Next, we analyze the *dynamic stability* of translation parallel to the wall. Consider the *linearization* of the discrete-time dynamics (4) under small deviations about the equilibrium point $\delta \mathbf{q}' = \mathbf{q}' - \mathbf{q}'_e$, which is given by

$$\delta \mathbf{q}'_{k+1} = \mathbf{A} \delta \mathbf{q}'_k, \text{ where } \mathbf{A}_{2 \times 2} = \left. \frac{\partial \mathcal{F}'}{\partial \mathbf{q}'} \right|_{\mathbf{q}' = \mathbf{q}'_e}.$$

The stability of \mathbf{q}'_e is determined by the (complex) eigenvalues of the linearization matrix \mathbf{A} , as follows. If all eigenvalues have magnitudes less than one, then \mathbf{q}'_e is asymptotically stable. If one or more eigenvalues have magnitudes greater than one then \mathbf{q}'_e is unstable. The equilibrium points of the form $\mathbf{q}'_e = (y_e, 0)$ discussed above are called *reversible equilibria* since they are invariant under the reflection symmetry, i.e. $\mathbf{M}'_q \mathbf{q}'_e = \mathbf{q}'_e$. Due to the reversing symmetry of (4), it is shown in [14] that the linearization eigenvalues must be a reciprocal pair $\{\lambda, \lambda^{-1}\}$. In the case of real eigenvalues, one of them generally has a magnitude greater than one, hence \mathbf{q}'_e is unstable. In the case of complex eigenvalues, they must be a complex conjugate pair $\lambda_{1,2} = e^{\pm i\omega}$, that is, they both have magnitude equal to one. In this case, the reversing symmetry implies that \mathbf{q}'_e is *marginally stable*, and under small perturbations about \mathbf{q}'_e , the resulting trajectories \mathbf{q}'_k are nearly-periodic and form *invariant circles*, which are the discrete-time analogue of continuous-time periodic solutions (just like the fact that the continuous function $\sin(\omega t)$ is periodic but the discrete series $\sin(k\omega T)$ for $k \in \mathbb{N}$ is not periodic if $\omega T/\pi$ is irrational). As an example, consider again the chain-of-spheres three-link swimmer under a square gait of amplitude $\alpha = 60^\circ$ and shift $\beta = -1.276^\circ$, corresponding to an equilibrium point $\mathbf{q}'_e = (10, 0)$. Figs. 3(a)-(b) show the simulated discrete-time solution of (4) under initial conditions $\mathbf{q}'(0) = (14, 0^\circ)$. Fig. 3(c) shows motion snapshots of the swimmer at times $t = 15kT$. Note the remarkable similarity to the periodic solutions obtained for

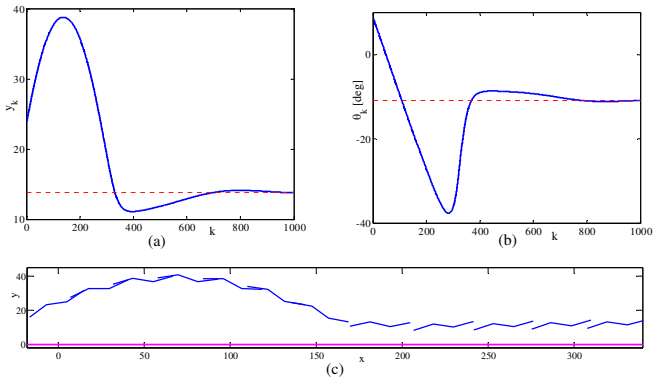


FIG. 4: Simulation of the non-symmetric gait. (a) Plot of y_k . (b) Plot of θ_k . (c) Snapshots of the swimmer's motion near the wall.

the fixed-shape swimmer model in [12].

In order to obtain *asymptotically stable* equilibrium solutions, the next step is to break the reversing symmetry of the system by changing the prescribed gait $\mathbf{s}(t)$ in a way that violates the relation (6). Due to the continuity of $\mathbf{G}'(\cdot)$ and $\mathcal{F}'(\cdot)$, under small changes in the gait $\mathbf{s}(t)$, the discrete-time map $\mathcal{F}'(\cdot)$ will also have a fixed point $\mathbf{q}'_e = (y_e, \theta_e)$ with $\theta_e \neq 0$, which is shifted from the original reversible equilibrium point. The eigenvalues of the linearization matrix \mathbf{A} about \mathbf{q}'_e also shift continuously from the original eigenvalues. In case where the original eigenvalues were a complex conjugate pair with unit magnitude, they will now be shifted as a complex conjugate pair. If their magnitude is less than one, \mathbf{q}'_e becomes stable, and if it is greater than one, \mathbf{q}'_e becomes unstable. However, playing the same gait backwards in time $\mathbf{s}(t) \rightarrow \mathbf{s}(T-t)$ will simply result in inversion of the discrete-time dynamics $\mathcal{F} \rightarrow \mathcal{F}^{-1}$, and of the corresponding eigenvalues $\lambda \rightarrow \lambda^{-1}$. That is, under the modified gait the swimmer has a *preferred swimming direction* for which swimming parallel to the wall becomes asymptotically stable. In the case of the square gait, the simplest way for breaking its reversing symmetry is to shift the entire square loop in (ϕ_1, ϕ_2) -plane in an amount of γ along the diagonal line $\phi_1 = -\phi_2$ [Fig. 2(c)]. As an example, we simulate the motion of the chain-of-spheres three-link swimmer under the square gait with amplitude $\alpha = 60^\circ$, shift of $\beta = -1.276^\circ$ along the line $\phi_1 = \phi_2$ and shift of $\gamma = 48^\circ$ along the line $\phi_1 = -\phi_2$, where the starting point $\mathbf{s}(0)$ is the bottom right corner of the square in (ϕ_1, ϕ_2) -plane. This gait corresponds to an equilibrium point $\mathbf{q}'_e = (13.8, -10.9^\circ)$ and linearization eigenvalues $\lambda_{1,2} = 0.9943e^{\pm 0.012i}$. Figs. 4(a)-(b) plot the discrete-time series of y_k and θ_k for initial condition $\mathbf{q}'(0) = (24, 8.6^\circ)$, and Fig. 4(c) plots motion snapshots of the swimmer at times $t = 50kT$ in xy plane. It can be seen that the swimmer converges passively to steady translation parallel to the wall. Remarkably, the stability

is achieved in *open loop* without applying any position sensing and feedback control. As a final remark, note that due to the time-invariance of (1) the results do not depend on the time parametrization of the gait $\mathbf{s}(t)$ but only on the geometric shape of its trajectory. Moreover, the stability characterization of parallel translation under a fixed gait do not depend on the choice of the starting point along the gait $\mathbf{s}(0)$, as illustrated in the simulation in Fig. 4 where a different starting point was chosen.

In summary, we analyzed the dynamics and stability of a chain-of-spheres version of Purcell's three-link low- Re swimmer near a plane wall. Using geometric symmetries of the dynamic equations, we have shown that it is possible to obtain a motion of net parallel translation which is dynamically stable, so that the swimmer is attracted to a fixed distance from the wall. The results agree with experiential observations on the wall-attraction of swimming bacteria and sperm cells. Importantly, the results are strongly based on analysis of the geometric structure of the dynamic equations, and do not depend of the exact details of the hydrodynamic model. In future work, it is planned to demonstrate the results experimentally on a robotic swimmer and to develop a more reliable numerical model for simulations and detailed parametric investigation.

The author deeply thanks Richard Murray from Caltech for fruitful discussions which initiated this study.

* izi@tx.technion.ac.il

- [1] E. Lauga and T. R. Powers, Rep. Prog. Phys. **72**, 096601 (2009).
- [2] J. E. Avron, O. Kenneth, and D. H. Oakmin, New J. Phys. **7**, 234238 (2005); A. Najafi and R. Golestanian, Phys. Rev. E **69**, 062901 (2004).
- [3] E. M. Purcell, Am. J. Phys. **45**, 3 (1977).
- [4] L. E. Becker, S. A. Koehler, and H. A. Stone, J. Fluid Mech. **490**, 15 (2003).
- [5] D. Tam and A. E. Hosoi, Phys Rev. Lett. **98**, 068105 (2007).
- [6] J. E. Avron and O. Raz, New J. Phys. **10**, 063016 (2008).
- [7] E. Lauga et al., Biophys. J. **90**, 400 (2006); K. Drescher et al., Phys Rev. Lett. **102**, 168101 (2009).
- [8] P. Frymier et al., Proc. Natl. Acad. Sci. **92**, 6195 (1995); J. Cosson, P. Huitorel, and C. Gagnon, Cell Motil. Cytoskeleton **54**, 56 (2003); A. P. Berke et al., Phys Rev. Lett. **101**, 038102 (2008).
- [9] T. Nakai, M. Kikuda, Y. Kuroda, and T. Goto, Journal of Biomechanical Science and Engineering **4**, 2 (2009).
- [10] M. Ramia, D. L. Tullock, and N. Phan-Thien, Biophysical Journal **65**, 755 (1993); L. J. Fauci and A. McDonald, J. Bull. Math. Biol. **57**, 679 (1995); H. Shum, E. A. Gaffney, and D. J. Smith, Proc. Roy. Soc. A (2010, online).
- [11] R. Zargar, A. Najafi, and M. Miri, Phys. Rev. E **80**, 026308 (2009).
- [12] Y. Or and R. M. Murray, Phys. Rev. E **79**, 045302(R) (2009).

- [13] S. Zhang, Y. Or, and R. M. Murray, in *Proc. American Control Conference* (2010), pp. 4205–4210.
- [14] J. S. W. Lamb and J. A. G. Roberts, *Physica D* **112**, 1 (1998); R. L. Devaney, *Trans. Am. Math. Soc.* **218**, 89 (1976).
- [15] A. Shapere and F. Wilczek, *J. Fluid Mech.* **198**, 557 (1989).
- [16] D. F. Katz, J. R. Blake, and S. L. Paverifontana, *J. Fluid Mech.* **72**, 529 (1975).
- [17] J. W. Swan and J. F. Brady, *Phys. Fluids* **19**, 113306 (2007).
- [18] Supplemental material is submitted as an additional file that will appear at the EPAPS electronic depository